Reverse Saturation Current Analysis in Photovoltaic Cell Models

JOSEAN RAMOS-HERNANZ[1], JOSE MANUEL LOPEZ-GUEDE[2], EKAITZ ZULUETA[2], UNAI FERNANDEZ-GAMIZ[3]
[1]Electrical Engineering Department, University of the Basque Country (UPV/EHU), Nieves Cano, 12, 01006 Vitoria-Gasteiz, SPAIN
[2]System Engineering & Automation Control Department, University of the Basque Country (UPV/EHU), Nieves Cano, 12, 01006 Vitoria-Gasteiz
[3]Department of Nuclear and Fluid Mechanics, University of the Basque Country (UPV/EHU), Nieves Cano, 12, 01006 Vitoria-Gasteiz, SPAIN
josean.ramos@ehu.eus, jm.lopez@ehu.eus, ekaitz.zulueta@ehu.eus, unai.fernandez@ehu.eus

Abstract: - In the scope of Photovoltaic energy it is very important to have precise models for simulation in order to know performance of a cell or photovoltaic module, in such a way that it is possible to test their behavior. Modeling the reverse saturation current is not a trivial task, and there is a number of different approaches carried out by several authors. In this paper we present an analysis of the different models of the literature to study the behavior of the reverse saturation current. In order to get it, some simulations have been carried out in Matlab/Simulink, where the different definitions of the reverse saturation current have been used, obtaining different predicted results and discussing them, being the most outstanding conclusion that actually there are only two different kinds of models.

Key-Words: - Photovoltaic (PV) - Photovoltaic module - Diode - Reverse saturation current - Matlab/Simulink.

1 Introduction

Due to the versatility of photovoltaic installations, the increase in the efficiency of the photovoltaic modules, together with a substantial decrease in price worldwide, photovoltaic energy is today a competitive sector, being able to adapt to any location, in a world where there are still many regions that do not have access to electricity.
Photovoltaic energy has already reached a high degree of maturity, although it still has a room for improvement. Thus, this paper carries out an analysis of photovoltaic technology. In particular, it analyzes the reverse saturation current produced in the photovoltaic cell.
The goodness of a simulation model of a photovoltaic module lies in verifying that the simulated data match the data provided by the manufacturer under standard test conditions, or fit to the measurements gathered experimentally in the actual photovoltaic module.
There are two general ways of developing these models. The first is to develop the models from equations that define the behavior of the photovoltaic modules. The second is based on real modules, doing experimental measurements and using them to obtain the model through approximations.
When authors develop their models from equations, not all of them agree on these equations. Therefore, in this paper, we analyze those differences, in particular the different equations that the authors use to define the reverse saturation current produced in the photovoltaic cells.
A photovoltaic module is formed by the connection of multiple solar cells connected in series and/or in parallel to obtain the desired voltage and current. A solar cell is a semiconductor system that absorbs light (solar energy) and converts it directly into electrical energy. The main source of energy of a photovoltaic system is the photovoltaic cell. For this reason, a photovoltaic generator is constituted of many solar cells associated electrically among them.
The most common photovoltaic cell consists of a thin sheet of semiconductor material, composed mainly of silicon of a specific degree of purity, which when exposed to sunlight absorbs photons of light with sufficient energy to cause the “electron hopping”, moving them from their original position towards the illuminated surface. When these electrons move with their negative charge (n) they generate holes with positive charges (p).
The ideal solar cell theoretically can be modeled as a current source with an anti-parallel diode (see Fig. 1). Direct current, generated when the cell is exposed to light, varies linearly with the solar

radiation. An improvement of the model includes the effect of a shunt resistor and other one in series.
Photovoltaic panels are the electricity generating elements. They are composed of rows and columns of photovoltaic cells that are connected in an array form whose parameters are directly proportional to

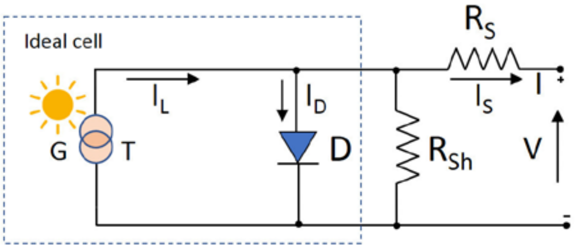

Fig. 1. Equivalent circuit for PV cell

the number of cells and the parameters of each one of the cells.
Based on the equivalent circuit of a p anel or photovoltaic cell (Fig. 1) the characteristic equation that gives the relationship between the voltage at its terminals and the current supplied is the following:

$$I = I_L - I_D - I_P \tag{1}$$

$$I = I_L - I_0\left(e^{\frac{q(V+IR_S)}{AKT}} - 1\right) - \frac{(V + IR_S)}{R_{SH}} \tag{2}$$

The net current produced is the photocurrent I_L (the current generated by the incident light, directly proportional to the solar irradiation) minus I_D (the diode current) and minus the current due to losses I_P, as shown in Eq. (1).
On the other hand, Eq. (2) describes the electrical behavior and determines the relationship between voltage and current supplied by a photovoltaic module, where $\mathbf{I_L}$ is the current produced by the photoelectric effect (A), $\mathbf{I_0}$ is the reverse bias saturation current (A), **V** is cell voltage (V), **q** is the charge of an electron equal to $1.6x10^{-19}$ (C), **A** is the diode ideality constant, **K** is the Boltzan's constant $1.38x10^{-23}$ (j/K), **T** is the absolute temperature of the junction, $\mathbf{R_S}$ and $\mathbf{R_{SH}}$ are the inherent resistances in series and in shunt to the cell associated.
The series resistance R_S is due to the load resistance of the semiconductor material, the metal contacts and interconnects and contact resistances between the semiconductor and the metal contacts. The shunt resistance R_{SH} is due to non-idealities and impurities near the PN junction.
As the solar cell is only capable of generating very low terminal voltage and output current, for the working purposes many cells are connected in series to form higher voltage across the terminal and connected in parallel to form a module. For large scale operation of PV generator, modules are connected in series and parallel to form arrays.
To determine the behavior of the solar panels it is necessary to know the voltage and amperage provided by different operating states in which they may work.
To use Eq. (2) it is necessary to know the value of R_S and R_{SH} resistors, characteristic parameters of each panel and the diode ideality factor, *a*. These parameters are related to the material used in its manufacture and in general are to be calculated since the manufacturer does not provide this information. Once calculated they are considered constant throughout the operating range and for any value of irradiation and temperature. It is also important to know the behavior of the reverse saturation current, I_0. In this term the authors do not agree, being several the equations used for their modeling.
Therefore, in this paper the most commonly used definitions and their influence on the final result is discussed.
The paper is structured as follows: in Section 2 an overview of basic concepts used in this work is given, section 3 reviews different models of inverse saturation current, while section 4 s hows and discuss the comparisons among the different models, while finally, our conclusions are given in section 5.

2 Background

2.1 Diode

The basic model of a photovoltaic generator is a solar cell. The solar cell can be analyzed as a diode, usually of silicon, designed to maximize photon absorption and minimize reflection, directly transforming part of the solar energy received into electrical energy.
The ideal diode is a discrete device that allows current flow between its terminals in a single direction, while locking it in the opposite direction.
In Fig. 2, shows the symbol and the voltage-current characteristic curve of the operation of the ideal diode. The allowed direction for the current is from

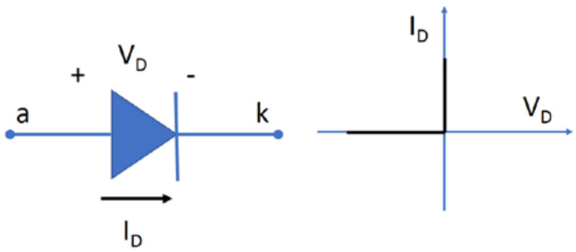

Fig. 2. Symbol and voltage-current characteristic curve of ideal diode

anode (a) to cathode (k). In conduction the anode-cathode-voltage is positive $V_{AK}>0$.
The ideal diode is a component that presents zero resistance to the cross of the current in a certain direction and infinite resistance in the opposite direction; in this case it behaves as open circuit.
The expression shown by Eq. (3) is a mathematical model that approximates properly the behavior of the real diode:

$$I_D = I_0\left(e^{\frac{V_D}{AV_T}} - 1\right) \qquad V_T = \frac{KT}{q} \tag{3}$$

where $\mathbf{I_D}$ is the current through the diode (A), $\mathbf{I_0}$ is the reverse bias saturation current (A), $\mathbf{V_D}$ is the voltage on the diode (V), $\mathbf{V_T}$ is the thermal voltage of the diode (V), which at room temperature (T = 25 ^{o}C) has a value of 25.71 mV, **q** is the charge of an electron equal to $1.6\text{x}10^{-19}$ (C), **A** is the diode ideality constant, **K** is the Boltzan's constant $1.38\text{x}10^{-23}$ (j/K), **T** is the absolute temperature of the junction

2.2 Reverse polarization

When applying a positive voltage to the cathode and negative to the anode, they are withdrawn the majority carriers close to the union. These carriers are attracted to the contacts by increasing the width of the depletion zone and the current due to the majority carriers is null:

- The positive pole of the power supply attracts free electrons from zone n, which come out of the crystal n and are inserted into the conductor into which they move until they reach the battery.
- The negative pole of the battery yields free electrons to the trivalent atoms of zone p.

In this situation, the diode should not conduct current; however, due mainly to the effect of the temperature it will be formed by breakages links, electron-hole pairs on both sides of the union, producing a small current (of the order of 1 μA) called *reverse saturation current*. If a specific voltage value is exceeded, then it is produced an abrupt conduction effect that can deteriorate the diode.
For reverse polarization, $V_D < 0$, the current is very small and the PN junction is not conductive.
Then we can define *Reverse Saturation Current* (I_0) as a small current that is established by inversely polarizing the diode by the formation of electron-hole pairs. It depends on doped levels, diode geometry and temperature, which approximately doubles every ten Celsius degrees. It should be noted that at a temperature of 300K the voltage drop at the junction decreases with the temperature in 2.2 mV/^{o}C, which partially compensates the increase of I_0.
This reverse current is negligible on most occasions, but it should be taken into account to prevent undesired operations.

3 Reverse Saturation Current Models

Authors do not agree how to mathematically define the reverse saturation current for the modeling of a photovoltaic cell, having different models.
In this section some modes of the literature are reviewed, and reference is made to only some of the authors who use each models.

3.1 Model 1

This model is used in [6], [8], [11], [17] and [19], defining the reverse saturation current by Eq. (4):

$$I_0 = I_0(T_{ref})\left(\frac{T}{T_{ref}}\right)^{\frac{3}{A}} e^{\frac{-qE_g}{AK}\left(\frac{1}{T}-\frac{1}{T_{ref}}\right)} \tag{4}$$

In [8] when authors describe the computer program used, they specify that they use this equation. However, it does not agree with the equation that it names when it does the theoretical development. It is the same than used in [17].
In [19] authors say that they use this equation like [24], but when they write it they introduce a T_2 term. We assume that there may be a transcription error.

3.2 Model 2

This model is used in [2], [3], [9], [14], [18], [20] and [21], defining the reverse saturation current by Eq. (5):

$$I_0 = I_0(T_{ref})\left(\frac{T}{T_{ref}}\right)^3 e^{\frac{qE_g}{AK}\left(\frac{1}{T_{ref}}-\frac{1}{T}\right)} \tag{5}$$

When [20] describes the used computer program, a very similar equation is used, but it is not divided by K.

3.3 Model 3

This model is used in [10], [22] and [23], defining the reverse saturation current by Eq. (6):

$$I_0 = I_0(T_{ref})\left(\frac{T_{ref}}{T}\right)^3 e^{\frac{qE_g}{AK}\left(\frac{1}{T_{ref}}-\frac{1}{T}\right)} \tag{6}$$

3.4 Model 4

This model is used by the same author in two different papers, [15] and [16], defining the reverse saturation current as defined by Eq. (7)

$$I_0 = I_0(T_{ref})\left(\frac{T}{T_{ref}}\right)^3 e^{\frac{qE_g}{AKT_{ref}}\left(\frac{T}{T_{ref}}-1\right)} \tag{7}$$

3.5 Model 5

This model is used in [1], [7], [12] and [13], defining the reverse saturation by Eq. (8):

$$I_0 = I_0(T_{ref})\left(\frac{T}{T_{ref}}\right)^3 e^{\frac{N_S E_g}{A_{ref}}\left(1-\frac{T_{ref}}{T}\right)} \tag{8}$$

In [1] and [12] instead of using A_{ref} , $A = A_{ref}\,(T/T_{ref})$ is used. In [7] authors multiply A_{ref} by the value of the load, *q*.

3.6 Model 6

This model is used in [5], defining the reverse saturation by Eq. (9):

$$I_0 = I_0(T_{ref})\left(\frac{T}{T_{ref}}\right)^3 e^{\frac{1}{K}\left(\frac{E_g}{T_{ref}}-\frac{E_g}{T}\right)} \tag{9}$$

The works of [4] and [5] belong to the same author. In [4] he uses the Model 5, while in other papers like in [5] he uses the equation defined by Eq. (9).

4 Comparison of models

Model 2 is the model used as reference because it is used by the larger number of researchers. Basing our comparisons on this model, we analyze the positive (yellow) or negative (blue) percentage variation of each model of the remaining.
For comparing the models, a photovoltaic system is modeled in which the model to be analyzed is included.
First the irradiance is fixed and the temperature is changed.

Model	Power (W)	20R%
Model 1	193,63	0,368
Model 2	192,92	0
Model 3	191,2	-0,892
Model 4	185,98	-3,597
Model 5	192,85	-0,036
Model 6	198,54	2,913

Table 1. Results for an Irradiance of 1000 W/m^2 and Temperature of 20 °C

For an Irradiance of 1,000W/m^2 and Temperature of 20 °C the values shown in Table 1 are obtained, where Model 2 is the reference, and the cells in blue indicate that the obtained value is smaller than the reference, while the yellow ones that the value is larger.
Fig. 3 is more complete, showing the values of the percentage of increment or decrement of each model for different temperatures (20, 30 and 40 °C) and for an irradiance of 1000 W/m^2. Due to space issues, Table 1 shows only the numeric values for 20 ºC.

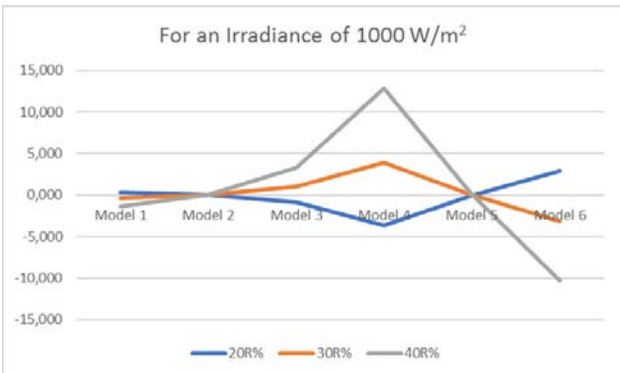

Fig. 3. Comparison among models

Model 2 and Model 5 give a very similar result, being the models that most differ the Models 4 and Model 6.
For an Irradiance of 600W/m^2 and Temperature of 20 ºC the values shown in Table 2 are obtained, where Model 2 is the reference.

Model	Power (W)	20R%
Model 1	110,96	0,380
Model 2	110,54	0,000
Model 3	109,51	-0,932
Model 4	106,39	-3,754
Model 5	110,5	-0,036
Model 6	113,9	3,040

Table 2. Results for an Irradiance of 600 W/m^2 and Temperature of 20 ^{o}C

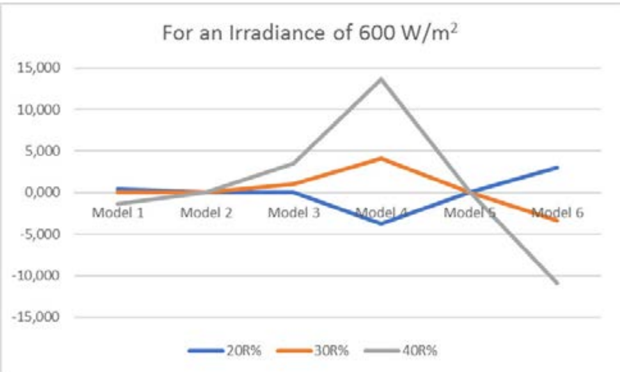

Fig. 4 Comparison among models

Fig. 4 is more complete, showing the values of the percentage of increment or decrement of each model for different temperatures (20, 30 and 40 ºC) and for an irradiance of 600 W/m^2. Due to space issues, Table 1 shows only the numeric values for 20 ºC.
In this situation also Model 2 and Model 5 give a very similar result and being, while again Model 4 and Model 6 vary their results.
In the other set of comparisons, the temperature is fixed and the irradiance is varied.
For a Temperature of 15 ºC and Irradiance of 900 W/m^2 the values shown in Table 3 are obtained, where Model 2 is the reference.
Fig. 5 is more complete, showing the values of the percentage of increment or decrement of each model

Model	Power (W)	900R%
Model 1	180,42	0,698
Model 2	179,17	0
Model 3	176,08	-1,725
Model 4	166,66	-6,982
Model 5	179,04	-0,073
Model 6	189,3	5,654

Table 3. Temperature of 15 ^{o}C and Irradiance of 900 W/m^2

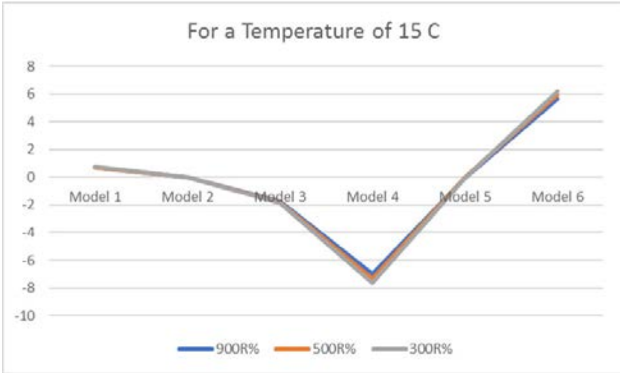

Fig. 5. Comparison among models.

Model	Power (W)	900R%
Model 1	133,66	-1,894
Model 2	136,24	0,000
Model 3	142,64	4,698
Model 4	161,11	18,255
Model 5	136,5	0,191
Model 6	116,49	-14,496

Table 4. Temperature of 45 ^{o}C and Irradiance of 900 W/m^2

for different irradiances (900, 500 and 300 W/m^2) and for a temperature of 15 ºC.
Due to space issues, Table 3 shows only the numeric values for irradiance of 900 W/m^2. Again Model 2 and Model 5 give a very similar result and the models that differ most are Models 4 and Model 6.
For a Temperature of 45 ºC and Irradiance of 900 W/m2 the values shown in Table 4 are obtained, where Model 2 is the reference.
Fig. 6 is more complete, showing the values of the percentage of increment or decrement of each model for different irradiances (900, 500 and 300 W/m2) and for a temperature of 45 ºC. Due to space issues, Table 4 shows only the numeric values for irradiance of 900 W/m2.
In this situation also Model 2 and Model 5 give a very similar result and being, while again Model 4 and Model 6 vary their results.

5 Conclusions

The model most similar to the model adopted as the base (Model 2 because it is used by more authors) is Model 5, being Model 4 and Model 6 the models that give a more different result.
It is noteworthy that, when we maintain fixed the temperature and irradiance varies, the percentages of the obtained results are kept very similar for all

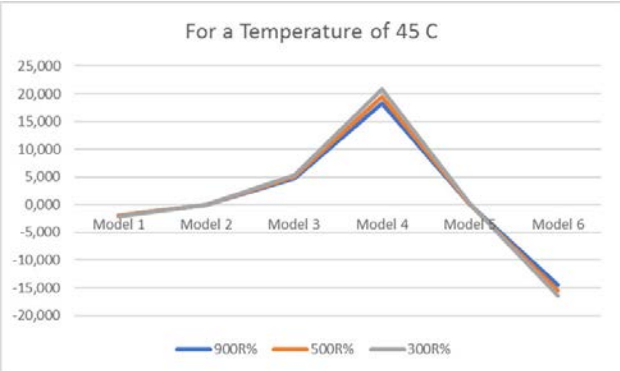

Fig. 6. Comparison among models

irradiances. However, when we fixed the irradiance and the temperature varies, it is observed that the temperature has a greater influence.

References:

[1] Celik, A. N., & Acikgoz, N. (2007). Modelling and experimental verification of the operating current of mono-crystalline photovoltaic modules using four-and five-parameter models. Applied energy, 84(1), 1-15.

[2] Chao, K. H., Ho, S. H., & Wang, M. H. (2008). Modeling and fault diagnosis of a photovoltaic system. Electric Power Systems Research, 78(1), 97-105.

[3] Chenni, R., Makhlouf, M., Kerbache, T., & Bouzid, A. (2007). A detailed modeling method for photovoltaic cells. Energy, 32(9), 1724-1730.

[4] De Soto, W. (2004). Improvement and Validation of a Model for Photovoltaic Array Performance (Doctoral dissertation, University of Wisconsin-Madison).

[5] De Soto, W., Klein, S. A., & Beckman, W. A. (2006). Improvement and validation of a model for photovoltaic array performance. Solar energy, 80(1), 78-88.

[6] DenHerder, T. (2006). Design and simulation of photovoltaic super system using simulink (Doctoral dissertation, California Polytechnic State University).

[7] Du, Y. F., & Mei, Y. (2011, September). Dynamic modeling and simulation of photovoltaic energy conversion system. In Wireless Communications, Networking and Mobile Computing (WiCOM), 2011 7 th International Conference on (pp. 1-6). IEEE.

[8] González-Longatt, F. M. (2005). Model of photovoltaic module in Matlab. Ii Cibelec, 2005, 1-5.

[9] Ikegami, T., Maezono, T., Nakanishi, F., Yamagata, Y., & Ebihara, K. (2001). Estimation of equivalent circuit parameters of PV module and its application to optimal operation of PV system. Solar energy materials and solar cells, 67(1), 389-395.

[10] Ishaque, K., Salam, Z., & Taheri, H. (2011). Accurate MATLAB simulink PV system simulator based on a two-diode model. Journal of Power Electronics, 11(2), 179-187.

[11] Kirar, J. S. (2013). Matlab Based Modelling of PV Array at Different Irrediation Level Using MPPT Technique.

[12] Kou, Q., Klein, S. A., & Beckman, W. A. (1998). A method for estimating the long-term performance of direct-coupled PV pumping systems. Solar Energy, 64(1), 33-40.

[13] Merino, G. G., Lagos, L. O., & Gontupil, J. E. (2008). Monitoring and evaluation of a direct coupled photovoltaic pumping system. Applied engineering in agriculture, 24(3), 277-284.

[14] Molina, M. G., & Espejo, E. J. (2014). Modeling and simulation of grid-connected photovoltaic energy conversion systems. International Journal of Hydrogen Energy, 39(16), 8702-8707.

[15] Nema, R. K., Nema, S., & Agnihotri, G. (2009). Computer simulation based study of photovoltaic cells/modules and their experimental verification. International Journal of Recent Trends in Engineering, 1(3).

[16] Nema, S., Nema, R. K., & Agnihotri, G. (2010). Matlab/simulink based study of photovoltaic cells/modules/array and their experimental verification. International journal of Energy and Environment, 1(3), 487-500.

[17] Oi, A. (2005). Design and simulation of photovoltaic water pumping system. California Polytechnic State University.

[18] Rustemli, S., & Dincer, F. (2011). Modeling of photovoltaic panel and examining effects of temperature in Matlab/Simulink. Elektronika ir Elektrotechnika, 109(3), 35-40.

[19] Sera, D., Teodorescu, R., & Rodriguez, P. (2007, June). PV panel model based on datasheet values. In Industrial Electronics, 2007. ISIE 2007. IEEE International Symposium on (pp. 2392-2396). IEEE

[20] Townsend, T. U., (1989), M.S. Thesis, Mechanical Engineering, U. of Wisconsin-Madison, “A Method for Estimating the Long-

Term Performance of Direct-Coupled Photovoltaic Systems”.

[21] Tsai, H. L., Tu, C. S., & Su, Y. J. (2008, October). Development of generalized photovoltaic model using MATLAB/SIMULINK. In Proceedings of the world congress on Engineering and computer science (Vol. 2008, pp. 1-6).

[22] Villalva, M. G., Gazoli, J. R., & Ruppert Filho, E. (2009). Comprehensive approach to modeling and simulation of photovoltaic arrays. IEEE Transactions on power electronics, 24(5), 1198-1208.

[23] Villalva, M. G., Gazoli, J. R., & Ruppert Filho, E. (2009, September). Modeling and circuit-based simulation of photovoltaic arrays. In Power Electronics Conference, 2009. COBEP'09. Brazilian (pp. 1244-1254). IEEE.

[24] Walker, G. (2001). Evaluating MPPT converter topologies using a MATLAB PV model. Journal of Electrical & Electronics Engineering, 21(1), 49-56.